

Supporting Information

Explorations of the Nonheme High-Valent Iron-Oxo Landscape: Crystal Structure of a Synthetic High-valent Complex with an $[\text{Fe}^{\text{IV}}_2(\mu\text{-O})_2]$ Diamond Core Related to the Chemistry of sMMOH

Gregory T. Rohde, Genqiang Xue, and Lawrence Que, Jr.

Department of Chemistry and Center for Metals in Biocatalysis, University of Minnesota,
Minneapolis, Minnesota 55455, USA

Table of Contents

Experimental Section	S2
Experimental Section References	S5
Table S1: EXAFS fitting to unfiltered EXAFS data of crystalline 1A, $[\text{Fe}^{\text{III}}_2(\mu\text{-O})(\mu\text{-OH})(\text{TPA}^*)_2]^{3+}$	S6
EXAFS analysis of crystalline 2A, $[\text{Fe}^{\text{III}}_2(\mu\text{-OH})_2(\text{TPA}^*)_2]^{4+}$	S7
Table S2. EXAFS fitting to unfiltered EXAFS data for crystalline $[\text{Fe}^{\text{III}}_2(\mu\text{-OH})_2(\text{TPA}^*)_2]^{4+}$ (2A)	S7
Table S3. EXAFS fitting to unfiltered EXAFS data for 2A, 5 mM solution of $[\text{Fe}^{\text{III}}_2(\mu\text{-O})(\text{OH})_2(\text{TPA}^*)_2]^{4+}$ (2A)	S8
Figure S1. Crystal structure of the trication of 3A, $[\text{Fe}^{3.5}_2(\mu\text{-O})_2(\text{TPA}^*)_2]^{3+}$,	S9
EXAFS analysis of 3A, $[\text{Fe}^{3.5}_2(\mu\text{-O})_2(\text{TPA}^*)_2]^{3+}$,	S10
Figure S2: Fourier-transformed Fe K-edge EXAFS data of $[\text{Fe}^{3.5}_2(\mu\text{-O})_2(\text{TPA}^*)_2]^{3+}$	S10
Table S4: EXAFS fitting to unfiltered EXAFS data of 3A $[\text{Fe}^{3.5}_2(\mu\text{-O})_2(\text{TPA}^*)_2]^{3+}$	S11
X-ray structure solutions and refinement details	S12
Figure S3: Packing diagram of $[\text{Fe}^3_2(\mu\text{-OH})_2(\text{TPA}^*)_2]^{4+}$ 2A	S13
Figure S4: Packing diagram of $[\text{Fe}^{3.5}_2(\mu\text{-O})_2(\text{TPA}^*)_2]^{3+}$ 3A	S14
Figure S5: Packing diagram of $[\text{Fe}^{\text{IV}}_2(\mu\text{-O})_2(\text{TPA}^*)_2]^{4+}$ 4A	S16
SI References	S17

Experimental Section

Materials and Synthesis

Anhydrous MeCN (>99.8%), 3-bromopyridine and 2,4,6-tri-tert-butylphenol were purchased from Aldrich and used as received. D₂O₂ (30% in D₂O, 98% D) was purchased from ICON Isotopes. 30% H₂O₂ in water and 70% H₂O₂ in H₂O were obtained from Macron and Degussa, respectively.

[Fe^{III}₂(μ-O)(μ-OH)(TPA*)₂](ClO₄)₃ (1A) was prepared according to the reported method.^a

[Fe^{III}₂(μ-OH)₂(TPA*)₂](ClO₄)₄•H₂O (2A) was prepared by adding a solution of 0.319 g (0.688 mmol) TPA* in 3 mL MeOH dropwise with stirring into a solution of 0.335 g Fe(ClO₄)₃•7.5H₂O in MeOH (0.688 mmol; the number of water molecules was calculated based on the iron content stated on the Aldrich Certification of Analysis). After the mixture was stirred for 2 h, 1.23 mL 0.500 M NaOH solution in MeOH (0.619 mmol) was added via syringe pump over a period of 1 hour. The mixture was further stirred at RT for another 5 hours, and 5 mL water was then added dropwise. A yellow powder formed upon stirring for 24 hours. The product was isolated by filtration and washed with 1:1 MeOH-H₂O containing 1 mM HClO₄. Yield: 0.51 g, 90% yield. Calcd. for [Fe₂(μ-O)(TPA*)₂(H₂O)₂](ClO₄)₄•H₂O (C₅₄H₇₈Cl₄Fe₂N₈O₂₆): C, 42.99; H, 5.21; N, 7.43; Cl, 9.40. Found: C, 43.13; H, 5.05; N, 7.44; Cl, 9.20. For recrystallization, 10 mg complex was dissolved in 0.5 mL MeCN to obtain a clear orange solution, which was placed in an Et₂O bath. Slight orange block-shaped crystals suitable for X-ray diffraction study, *vide infra*, were formed when about 0.5 mL Et₂O was diffused into the solution. The block was placed in inert oil and mounted on the diffractometer. Crystallographic data C₆₂H₈₈Cl₄Fe₂N₁₂O₂₅, *M* = 1653.05, triclinic, *a* = 11.6840(13) Å, *b* = 13.3450(15) Å, *c* = 25.013(3) Å, α = 75.1520(10)°, β = 84.9130(10)°, γ = 87.7530(10)°, *U* = 3754.5(7) Å³, *T* = 173 K, space group P-1 (no.2), *Z* = 1, 33117 reflections measured, 16744 unique (*R*_{int} = 0.0402), 10659 reflections *I* > 2σ(*I*), which were used in all calculations. *R*₁ [*I* > 2σ(*I*)] was 0.0575 and the final *R*_{all} was 0.1018. Goof 1.023, CCDC number 2111623.

[Fe^{III}Fe^{IV}(μ -O)₂(TPA*)₂](ClO₄)₃ • PrCN (3A) was prepared as previously reported except in a butyronitrile solution and then layering the solution with diethyl ether at -80°C.^a Dark green block crystals were obtained and placed in inert oil on a microscope slide that was precooled with liquid nitrogen to keep the crystals at low temperature during handling and mounting on the diffractometer. Crystallographic data: C₆₂H₉₀Cl₃Fe₂N₁₀O₂₂, *M* = 1545.48, monoclinic, *a* = 27.9262(12) Å, *b* = 11.1080(4) Å, *c* = 22.8446(10) Å, β = 105.110(3)°, *U* = 6841.5(5) Å³, *T* = 123 K, space group *C2/c* (no.15), *Z* = 4, 14758 reflections measured, 6021 unique (*R*_{int} = 0.0564), 3441 reflections *I* > 2σ(*I*), which were used in all calculations. *R*₁ [*I* > 2σ(*I*)] was 0.0875 and the final *R*_{all} was 0.1486. Goof 1.023, CCDC number 2111624.

[Fe^{IV}₂(μ -O)₂(TPA*)₂](ClO₄)₄•5.5 (PrCN) (4A) was prepared by initially dissolving 0.020 g (0.013 mmol) **2A** in 2 mL butyronitrile followed by the addition of 25 μL (1 eq.) of a 0.53 M solution of 3-bromopyridine in butyronitrile and then allowing the solution to cool to -80°C. After cooling, 40 μL (1 eq.) of a 0.34 M solution of H₂O₂ in 3:1 butyronitrile:-acetonitrile mixture (prepared from 70% H₂O₂ to minimize water) was added while swirling the vial to avoid pockets of high concentrations of H₂O₂ and side reactions. The solution immediately turned a dark red and was allowed to react for an additional 20 minutes at -80°C. After 20 minutes, 2 mL of diethyl ether at -80°C was layered on the solution and left for 7-10 days, after which red blocks-shaped crystals appropriate for X-ray diffraction studies were observed. The mother liquor from a separate batch was removed, washed with diethyl ether and then placed under vacuum for several hours all at -80°C. The dark red solid was dissolved in CD₃CN at -40°C and studied with UV-Vis, NMR and ESI-MS spectroscopies and matched previously reported values. The crystals were placed in inert oil on a microscope slide that was precooled with liquid nitrogen to keep the crystals at low temperature during handling and mounting on the diffractometer. Crystallographic data. C₁₅₂H₂₂₁Cl₈Fe₄N₂₇O₄₈, *M* = 3701.54, triclinic, *a* = 14.2183(9) Å, *b* = 15.7200(10) Å, *c* = 21.5627(13) Å, α = 86.579(4)°, β = 71.452(4)°, γ = 72.753(4)°, *U* = 4360.5(5) Å³, *T* = 123 K, space group *P*-1 (no.2), *Z* = 1, 27550 reflections measured, 7795 unique

($R_{\text{int}} = 0.1290$), 4485 reflections $I > 2\sigma(I)$, which were used in all calculations. $R_1 [I > 2\sigma(I)]$ was 0.0927 and the final R_{all} was 0.1626. Goof 1.025, CCDC number 2111625.

Physical Methods

Electronic absorption spectra were recorded on a Hewlett-Packard (Agilent) 8453A diode array spectrometer cooled using a liquid nitrogen cooled cryostat from Unisoku Scientific Instruments (Osaka, Japan). This combination allows kinetic studies to be performed at temperatures below $-85\text{ }^\circ\text{C}$ and to record a spectrum every 0.1 second. For rapid reactions with a reaction time of 10 seconds, time traces at one wavelength can be obtained with about 100 data points for reliable kinetic fits. Resonance Raman spectra were recorded on an Acton AM-506 spectrophotometer, using a Kaiser Optical holographic supernotch filter with a Princeton Instruments LN/CCD-1100-PB/UVAR detector cooled with liquid nitrogen. Laser excitation was provided by a Spectra Physics BeamLok 2060-RM argon ion laser. The spectra were obtained at 77 K by using a 135° -backscattering geometry, and the Raman frequencies were referenced to indene.

Iron K-edge X-ray absorption spectra were collected in fluorescence mode using a 30-element Ge detector on beamline X3B at the National Synchrotron Light Source at Brookhaven National Laboratory (NSLS). The synchrotron ring was operated at 2.8 GeV and 100-300 mA beam current and a Si(111) double crystal monochromator was used. The monochromator was calibrated to 7112.0 eV at the Fe K-edge using Fe foil. Samples were collected at 15-20 K over an energy range of 6.9-8.0 keV. Data were collected on frozen 5 mM acetonitrile solution samples of **2A** or a solid sample consisting of a 20:1 mixture of boron nitride and crystalline **2A**. The edge energies were routinely monitored during data collection for red-shifts indicative of sample photoreduction, but none were observed in the present study. Data reduction, averaging, and normalization were performed using the program EXAFSPAK.^b A three-segment spline with fourth order components was then fit to the EXAFS region of the spectrum in order to extract $\chi(k)$. Theoretical phase and amplitude parameters for a given absorber-scatterer pair were calculated using FEFF 8.40 and were utilized by the "opt" program of the EXAFSPAK package during curve-fitting. FEFF parameters for the solid and solution samples of **2A** were calculated using similar coordinates of the crystal reported above. In all analyses,

the coordination number of a given shell was a fixed parameter, and was varied iteratively while bond lengths (r) and mean square deviation (σ^2) were allowed to freely float. The amplitude reduction factor S_0 was fixed at 0.9, while the edge shift parameter E_0 was allowed to float as a single value for all shells (thus in any given fit, the number of floating parameters was typically equal to $(2 \times \text{num shells}) + 1$). The goodness-of-fit F was defined simply as $\sum (\chi_{\text{exptl}} - \chi_{\text{calc}})^2$. For fits to unfiltered data, a second goodness-of-fit parameter, F -factor, was defined as $[\sum k^6 (\chi_{\text{exptl}} - \chi_{\text{calc}})^2 / \sum k^6 \chi_{\text{exptl}}^2]^{1/2}$. In order to account for the effect that additional shells have on improving fit quality, a third goodness-of-fit metric F' was employed. $F' = F^2 / (N_{\text{IDP}} - N_{\text{VAR}})$, where N_{VAR} is the number of floated variables in the fit, while N_{IDP} is the number of independent data points and is defined as $N_{\text{IDP}} = 2\Delta k \Delta r / \pi$. In the latter equation, Δk is the k -range over which the data is fit, while Δr is the back-transformation range employed in fitting Fourier-filtered data. F' is thus of principal utility in fitting Fourier-filtered data, but can also be employed for unfiltered data by assuming a large value of Δr . Fitting tables are included below for the fit evaluation, with the best fit highlighted in yellow for each complex.

Experimental Section References:

- a. G. Xue, D. Wang, R. De Hont, A. T. Fiedler, X. Shan, E. Münck, L. Que, Jr., *Proc. Nat. Acad. Sci. USA* 2007, **104**, 20713.
- b. G. N. George, I. J. Pickering, EXAFSPAK, Stanford Synchrotron Radiation Laboratory, Stanford Linear Accelerator Center, Stanford, California, 2000.

Table S1: EXAFS fitting to unfiltered EXAFS data of crystalline **1A**, $[\text{Fe}^{\text{III}}_2(\mu\text{-O})(\mu\text{-OH})(\text{TPA}^*)_2]^{3+}$.

A 1:13 dilution of **1A**: BN crystalline sample was prepared and the data was analyzed using Feff phase and amplitude parameters listed in (Å).

Fit	Fe-N			Fe-O			Fe-C			Fe-Fe					
#	N	R	σ^2	N	R	σ^2	N	R	σ^2	N	R	σ^2	E_0	F	F'
Default phase and amplitude parameters															
1*	4	2.139	3.3	1	1.802	1.5	6	3.006	1.3	1	2.804	3.8	-5.63	124	386
				1	1.973	4.7									
2	4	2.123	3.2	2	1.829	9.3	6	2.996	1.6	1	2.793	3.5	-6.48	151	423

k range = 1-14 Å⁻¹, resolution = 0.12 Å, σ^2 = mean-squared deviation in units of 10⁻³ Å².

Scale Factor S_0^2 = 0.9. Goodness-of-fit = F calculated as $F = \sqrt{\sum k^6 (\chi_{\text{exp}} - \chi_{\text{calc}})^2}$.

$F' = \sqrt{\sum k^6 (\chi_{\text{exp}} - \chi_{\text{calc}})^2 / \sum k^6 \chi_{\text{exp}}^2}$. * = Best Fit

EXAFS analysis of crystalline **2A**, $[\text{Fe}^{\text{III}}_2(\mu\text{-OH})_2(\text{TPA}^*)_2]^{4+}$

The crystalline sample of **2A** presented some experimental challenges due to the fact that the distances of Fe•••C scatterers and the Fe•••Fe scatterer were within the resolution of the measurement and likely caused the negative Debye-Waller factors in Fit 6, Table S2. When the distance and Debye-Waller factors were set equal to each other (Fit 7, Table S2), a satisfactory Debye-Waller factor was obtained with an approximately average distance of the Fe•••C and Fe•••Fe scatterers. Therefore, in combination with the crystal structure, *vide infra*, the best fit is assigned to Fit 6.

Table S2. EXAFS fitting to unfiltered EXAFS data for crystalline $[\text{Fe}^{\text{III}}_2(\mu\text{-OH})_2(\text{TPA}^*)_2]^{4+}$ (**2A**) using Feff phase and amplitude parameters listed in Å.

Fit #	Fe-N			Fe-O			Fe•••C			Fe•••Fe			E_0	F	F'
	N	R	σ^2	N	R	σ^2	N	R	σ^2	N	R	σ^2			
Default phase and amplitude parameters															
1	4	2.113	2.2	2	1.939	5.1	4	2.957	1.4	1	3.017	1.4	-1.64	286	415
							6	3.108	1.1						
Feff		2.11			1.94			2.96, 3.11			3.04				
2	4	2.094	2.9	2	1.908	5.5							-11.4	863	721
3	5	2.077	4.5	1	1.874	1.3							-11.6	881	729
4	4	2.105	12.1	1	1.931	1.9							-7.13	832	708
				1	2.080	-1.8									
5	4	2.109	2.9	2	1.925	6.7	8	3.019	2.1				-7.22	355	462
6	4	2.098	2.3	2	1.911	5.4	4	2.945	-2.9	1	3.039	-1.2	-9.00	239	392
7	4	2.100	2.2	2	1.913	5.2	4	2.964	0.5	1	3.022 ^x	1.7	-8.93	246	398
8	4	2.101	2.5	2	1.913	5.8	6	3.001 ^f	3.7 ^f	1	3.001 ^f	3.7 ^f	-8.22	243	395

Adding a second Fe-C scatterer gave non-sensible distances with only a minor improvement in fit quality.

k range = 2-13.5 Å⁻¹, resolution = 0.137 Å, σ^2 = mean-squared deviation in units of 10⁻³ Å². Scale Factor

$S_0^2 = 0.9$. Goodness-of-fit = F calculated as $F = \sqrt{\sum k^6 (\chi_{\text{exp}} - \chi_{\text{calc}})^2}$.

$F' = \sqrt{\sum k^6 (\chi_{\text{exp}} - \chi_{\text{calc}})^2 / \sum k^6 \chi_{\text{exp}}^2}$. x = distance fixed from average bond distance in crystal structure. f = Fe-C and Fe•••Fe shells have their distance and Debye-Waller factors set equal to each other.

EXAFS analysis of 5 mM $[\text{Fe}^{\text{III}}_2(\mu\text{-O})(\text{OH}_2)_2(\text{TPA}^*)_2]^{4+}$ (**2A**) in MeCN sol'n**Table S3.** EXAFS fitting to unfiltered EXAFS data for **2A**, 5 mM solution of $[\text{Fe}^{\text{III}}_2(\mu\text{-O})(\text{OH}_2)_2(\text{TPA}^*)_2]^{4+}$ (**2A**) in MeCN using Feff phase and amplitude parameters listed in Å.

Fit #	Fe-N			Fe-O			Fe-C			Fe•••Fe			E_0	F	F'
	N	R	σ^2	N	R	σ^2	N	R	σ^2	N	R	σ^2			
Feff	2.11			1.79			3.03			3.419(m)					
1	5	2.096	3.9	1	1.784	0.8							-14.0	X	711
2	4	2.070	2.4	2	1.778	5.7							-20.8	X	750
3	5	2.111	4.1	1	1.790	0.3	8	3.021	3.8				-9.01	812	615
4	5	2.118	4.2	1	1.788	0.2	8	3.021	3.6	1	3.375	0.5	-7.42	614	534
5	5	2.118	4.3	1	1.789	0.0	8	3.030	2.6	1 4 ^m	3.418 3.569	0.1 0.8	-7.54	368	414
6	5	2.116	4.3	1	1.789	0.0	8	3.029	3.0	1 2 ^m	3.491 3.604	10.4 -2.7	-8.06	365	412
7	5	2.118	4.3	1	1.789	0.0	4 4	3.006 3.075	1.0 3.0	1 2 ^m	3.470 3.603	11.5 -2.5	-7.75	363	411
8	5	2.108	4.1	1	1.788	0.2	8 8	3.017 3.656	4.1 0.4	1	3.361	2.7	-9.80	392	427
9	5	2.058	3.8	1	1.761	1.0	8 1 ^m	3.246 3.509	-2.8 16.9	1	3.350	-3.6	-25.1	836	624

k range = 2-15 Å⁻¹, resolution = 0.122 Å, σ^2 = mean-squared deviation in units of 10⁻³ Å². Scale Factor S_0^2 = 0.9. Goodness-of-fit = F calculated as $F = \sqrt{\sum k^6 (\chi_{\text{exp}} - \chi_{\text{calc}})^2}$.

$F' = \sqrt{\sum k^6 (\chi_{\text{exp}} - \chi_{\text{calc}})^2 / \sum k^6 \chi_{\text{exp}}^2}$. ^m = multiple scattering pathway between Fe1-O1-Fe1A-Fe1.

As evident by the much improved quality factors going from Fit 4 to Fit 5 in Table S3, the additional multiple scattering pathway was necessary to obtain a satisfactory fit. Fits that included alternative multiple scattering pathways at different distances or fits that included a C atom, or additional Fe•••C shells did not provide a superior fit. Moreover, the calculated Fe–O–Fe bond angle is consistent with the symmetric and asymmetric vibrations observed in the resonance Raman spectrum of the iron-oxygen core. Therefore Fit 5 was chosen as the best fit in Table S3.

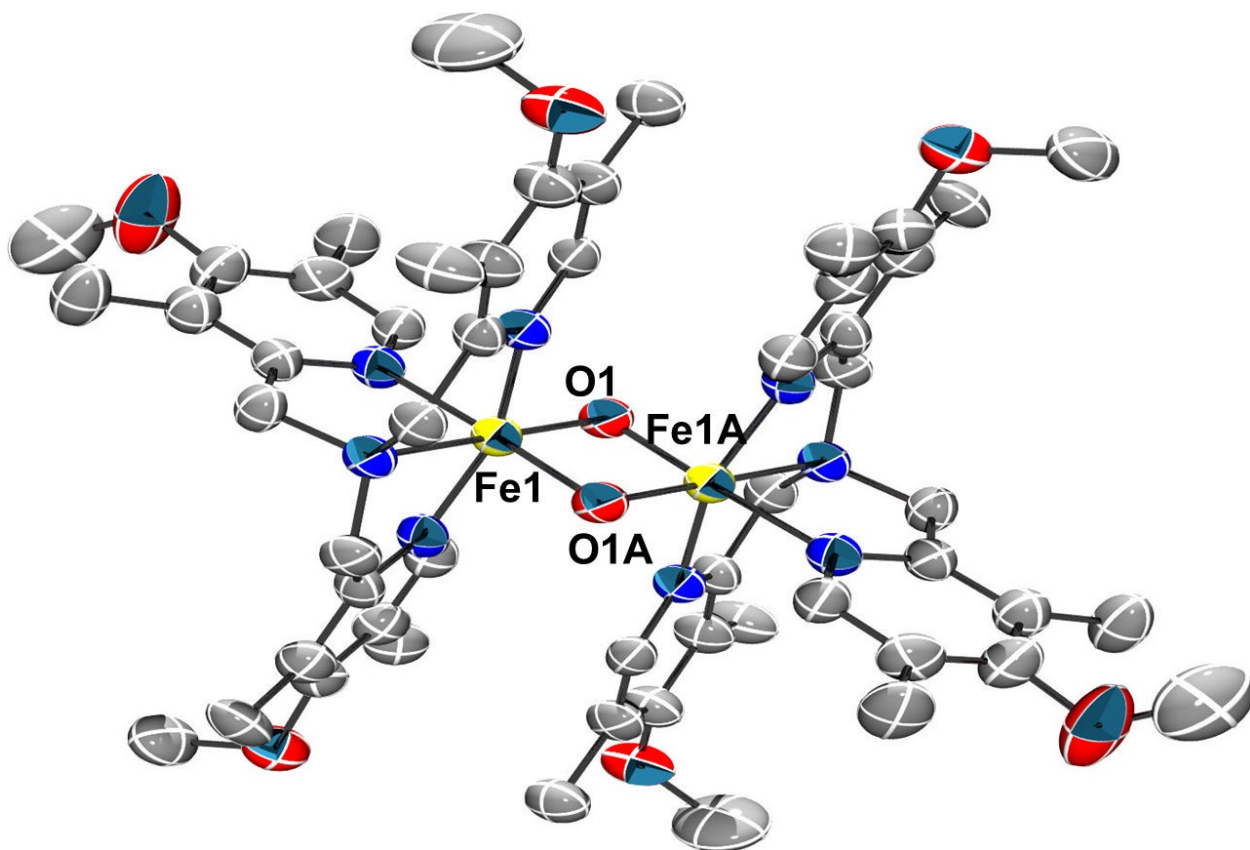


Figure S1. Crystal structure of the trication of **3A**, $[\text{Fe}^{3.5}_2(\mu\text{-O})_2(\text{TPA}^*)_2]^{3+}$, with thermal ellipsoids drawn to the 50% probability level. Perchlorate counterions, a butyronitrile solvent molecule, a water molecule and H-atoms were removed for clarity. Atom colors: carbon, gray; oxygen, red; nitrogen, blue; iron, yellow. An inversion center is present at the center of the Fe_2O_2 core of **3A**, making one half of the molecule unique. For a list of selected bond distances (Å) and angles ($^\circ$) for **3A** and related structures, see Table 2.

EXAFS analysis of **3A**, $[\text{Fe}^{3.5}_2(\mu\text{-O})_2(\text{TPA}^*)_2]^{3+}$, in frozen MeCN solution:

The 8 mM frozen MeCN solution sample of **3A** was analyzed by EXAFS and had similar structural parameters as the crystal structure. The EXAFS data and fitting table are displayed in Figure S2 and Table S4. Five scattering shells were fit to a k range of 2-14 \AA^{-1} including two Fe-O scatterers at 1.75 \AA , four Fe-N scatterers at 1.96 \AA , an Fe-Fe scatterer at 2.57 \AA and two sets of Fe-C scatterers at 2.77 and 2.92 \AA (Figure S2, Table S4, Fit 13), in reasonable agreement with the crystallographically determined distances. The intense scatterer at around 2.3 \AA in the Fourier transform has a major contribution from the Fe-Fe scatterer at 2.57 \AA and is consistent with the presence of a diamond core motif.

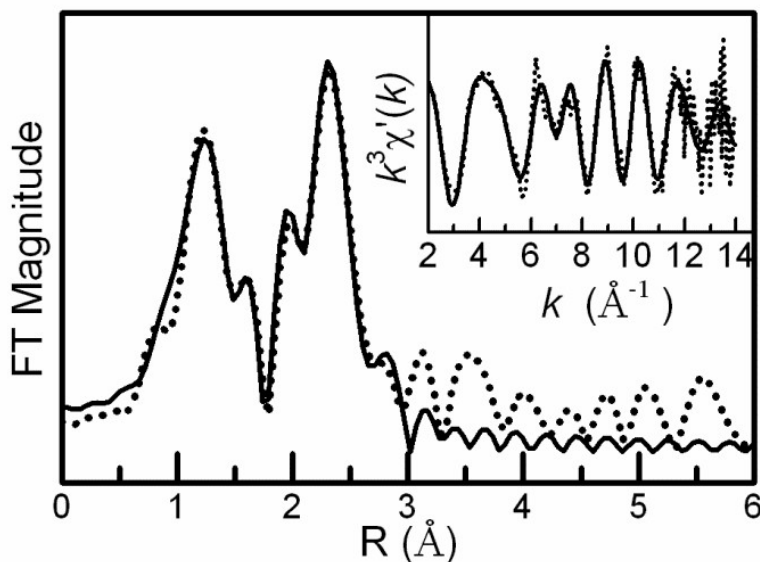


Figure S2: Fourier-transformed Fe K-edge EXAFS data of $[\text{Fe}^{3.5}_2(\mu\text{-O})_2(\text{TPA}^*)_2]^{3+}$.

Data obtained at 20 K of an 8 mM solution sample of **3A** in acetonitrile. (*Inset*) $k^3\chi'(k)$ data. Fourier transform range 2-14 \AA^{-1} ; experimental data (dotted line) and best fit (solid line), consisting of 1 O at 1.75 \AA , 3 N at 1.96 \AA , 1 Fe at 2.57 \AA and two additional Fe•••C shells at 2.77 and 2.93 \AA modeled with 4 and 6 scatterers, respectively.

Table S4: EXAFS fitting to unfiltered EXAFS data of **3A** $[\text{Fe}^{3.5}_2(\mu\text{-O})_2(\text{TPA}^*)_2]^{3+}$ using Feff phase and amplitude parameters listed in (Å).

Fit	Fe-N			Fe-O			Fe-C			Fe-Fe					
#	N	R	σ^2	N	R	σ^2	N	R	σ^2	N	R	σ^2	E_0	F	F'
Default phase and amplitude parameters from EXAFSPAK															
	3	1.971	5.9	2	1.771	6.3	3	2.801	1.4	1	2.590	2.8	-5.90	148	450
							4	2.961	0.5						
Feff	1.98			1.77			2.96,			2.59					
1	3	1.968	6.0	2	1.765	6.1							-13.0	468	802
2	4	1.962	8.6	2	1.754	6.4							-13.0	474	807
3	4	1.946	9.7	1	1.747	3.0							-11.3	467	801
4	3	1.968	6.1	2	1.766	6.1							-13.0	468	802
5	3	1.975	6.1	2	1.773	6.6	6	2.875	8.1	1	2.569	4.1	-10.4	193	515
6	3	1.967	6.3	2	1.766	6.8	6	2.932	2.7	1	2.562	3.6	-10.9	159	468
							6	2.768	4.7						
7	4	1.956	8.8	2	1.749	7.2	6	2.928	2.3	1	2.560	2.4	-11.6	172	487
							6	2.765	4.0						
8	4	1.937	9.5	1	1.738	3.2	6	2.936	2.4	1	2.565	2.4	-10.5	160	469
							6	2.771	4.2						
9	3	1.946	6.8	1	1.751	2.8	6	2.938	2.6	1	2.566	2.5	-9.9	153	458
							6	2.772	4.5						
10	3	1.948	6.7	1	1.752	2.8	6	2.929	2.2	1	2.573	2.4	-9.6	148	451
							4	2.770	1.2						
11	3	1.969	6.4	2	1.767	7.0	6	2.922	2.0	1	2.568	2.4	-10.7	156	463
							4	2.764	1.2						
12	4	1.940	9.5	1	1.740	3.2	6	2.935	2.0	1	2.570	2.4	-10.2	154	461
							4	2.767	1.1						
13*	4	1.961	8.9	2	1.753	7.3	6	2.922	1.7	1	2.569	2.4	-11.1	167	479
							4	2.767	0.8						

k range = 2-14 Å⁻¹, resolution = 0.132 Å, σ^2 = mean-squared deviation in units of 10⁻³ Å². Scale

Factor S_0^2 = 0.9. Goodness-of-fit = F calculated as $F = \sqrt{\sum k^6 (\chi_{\text{exp}} - \chi_{\text{calc}})^2}$.

$F' = \sqrt{\sum k^6 (\chi_{\text{exp}} - \chi_{\text{calc}})^2 / \sum k^6 \chi_{\text{exp}}^2}$. * = Best Fit

X-ray structure solutions and refinement details

For all three crystal structures reported herein, the crystals were mounted onto glass fibers or MiTeGen mounts and positioned on the diffractometer for a data collection with specific collection details in the experimental section of the main text below. A preliminary set of cell constants was calculated from reflections harvested from three sets of 12-20 frames. A randomly oriented region of reciprocal space was surveyed to the extent of one sphere consisting of four major sections of frames and was collected with 0.50° steps in ω at four different ϕ settings with a detector position of -28° in 2θ for the MoK α radiation collections for **2A**. A collection strategy was developed using the Queen program in the APEX II software suite to ensure full coverage for the Cu K α radiation collections for **3A** and **4A**.^{S1} The intensity data were corrected for absorption and decay with SADABS.^{S2} Final cell constants were calculated from the xyz centroids of strong reflections from the actual data collection after integration.^{S3} The space groups were determined based on systematic absences and intensity statistics with the program XPREP.^{S4} A direct-methods solution was calculated using SHELXS-97 (unless otherwise stated) which provided most non-hydrogen atoms from the E-map.^{S5} Full-matrix least squares / difference Fourier cycles were performed, which located the remaining non-hydrogen atoms. The atoms were refined as with anisotropic displacement parameters with hydrogen atoms riding with relative isotropic displacement parameters. The structures were initially refined using SHELXL-97 and further refined with shelXle.^{S5,S6} Specific refinement metrics are described in the experimental section of the main text.

Refinement details for 2A:

Solution of the crystal structure of complex **2A** was carried out in a routine manner as previously described. The packing diagram is displayed in Figure S3. All non-hydrogen atoms were refined with anisotropic displacement parameters. All hydrogen atoms bonded to carbon atoms were placed in ideal positions and refined as riding atoms with relative isotropic displacement parameters. Hydrogen atoms H1 and H1' were located on a difference Fourier map and refined with isotropic displacement parameters.

Hydrogen atoms H2O and H3O were located on a difference Fourier map and refined as riding atoms at 0.85 Å with relative isotropic displacement parameters. The methyl group bonded to O2 was modeled over two positions (55:45). Four acetonitrile molecules were located in the asymmetric unit and one of acetonitrile molecules was modeled over two positions (77:33). Four disordered perchlorate ions were modeled as perfect tetrahedrons over at least two positions in the asymmetric unit and their occupancies were allowed to refine freely. The μ -hydroxo ligand had disordered H-bonded acceptors and H-bonded to the O21 water molecule and a perchlorate counter ion in a 90:10 ratio, respectively.

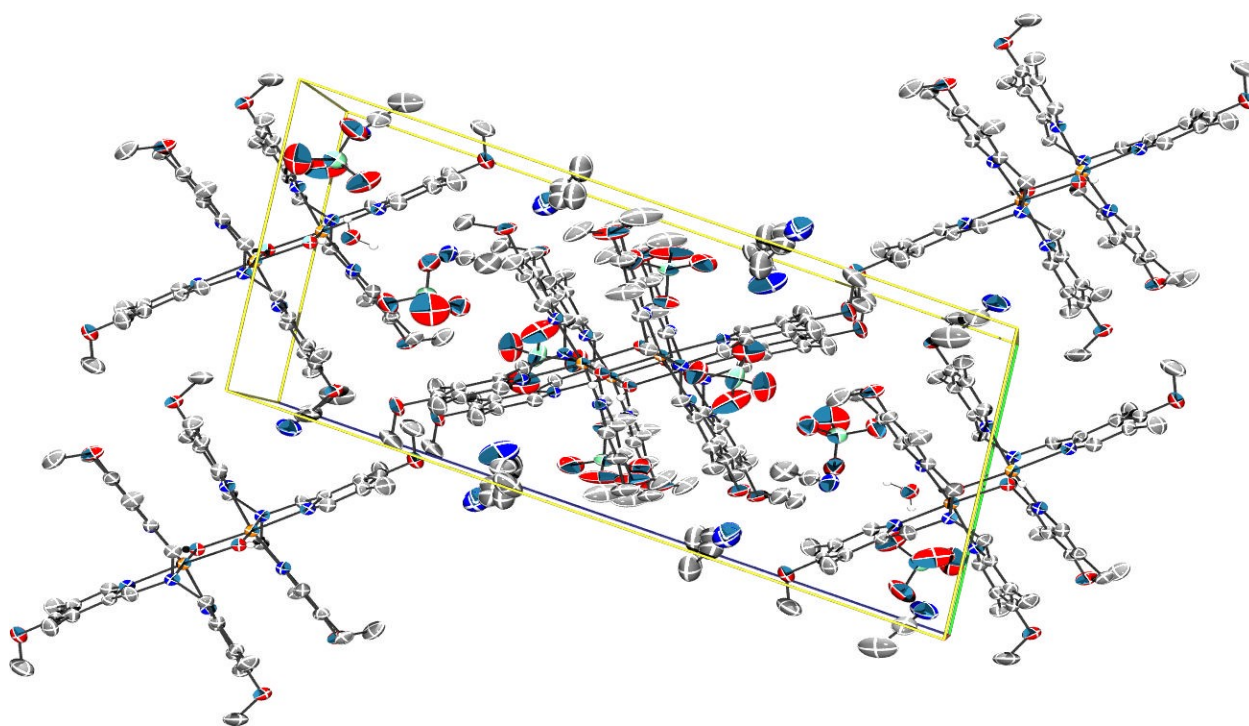


Figure S3: Packing diagram of $[\text{Fe}_2(\mu\text{-OH})_2(\text{TPA}^*)_2]^{4+}$ **2A** looking down the a-axis. Non-oxygen hydrogen atoms are removed for clarity. Atoms are drawn at the 50% probability level. Acetonitrile solvent molecules, water and perchlorate counter ions are visible in the cell. Atom colors: carbon- gray, oxygen- red, nitrogen- blue, iron- yellow, chlorine- green.

Refinement details for **3A**:

Solution of the crystal structure of complex **3A** was carried out in a routine manner as previously described, except that it was solved using SIR2011.⁷ The packing diagram is displayed in Figure S4. Additionally, one water molecule was located in the unit cell and H-bonded to perchlorate counter anions. The two water hydrogens were first located on a difference map and then refined as riding atoms with relative isotropic displacement parameters. All non-water hydrogen atoms were placed in ideal positions and refined as riding atoms with relative isotropic displacement parameters. The two perchlorate counterions and the butyronitrile molecule were modeled over two positions with occupancy ratios of 91:9, 91:9 and 69:31 respectively. All atom pairs in the disordered anions and solvent molecules were constrained to have the same anisotropic displacement parameters (EADP),⁵ and restrained to have all bond distances the same (SAME).⁵ All perchlorate ions and butyronitrile molecules were refined in a similar manner as discussed in the refinement of **4A**.

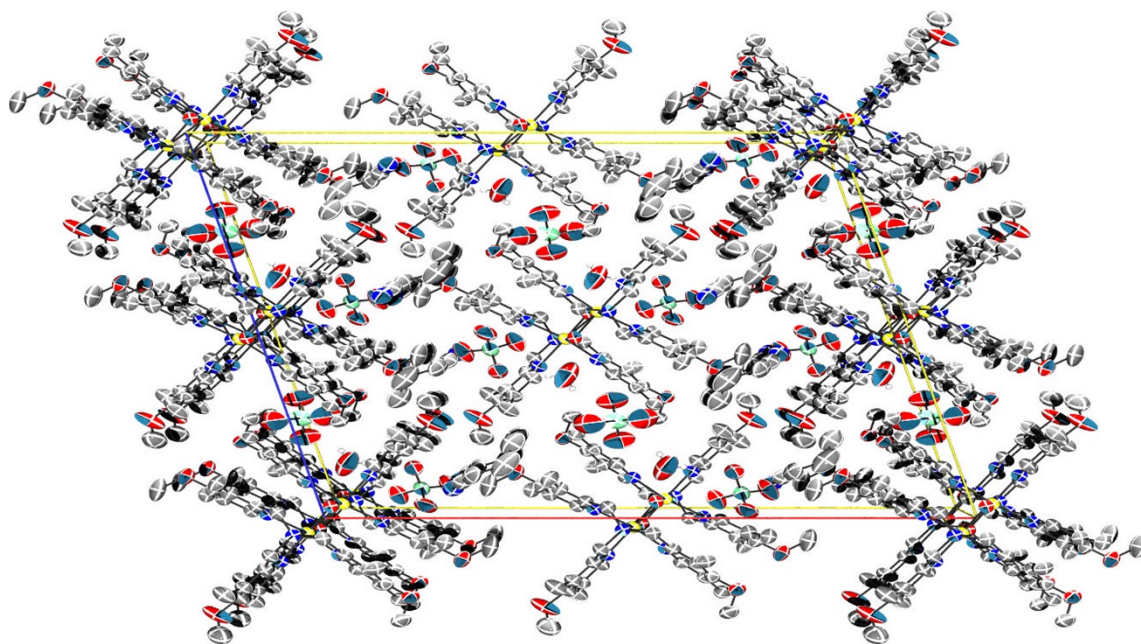


Figure S4: Packing diagram of $[\text{Fe}^{3.5}_2(\mu\text{-O})_2(\text{TPA}^*)_2]^{3+}$ **3A** looking down the b-axis. Hydrogen atoms are removed for clarity. Atoms are drawn at the 50% probability level. Butyronitrile solvent molecules, water and perchlorate counter ions are visible in the cell. Atom colors: carbon- gray, oxygen- red, nitrogen- blue, iron- yellow, chlorine- green.

Refinement details for 4A:

Refinement of complex **4A** was carried out in a routine manner as previously described. The packing diagram is displayed in Figure S5. Additionally, two distinct halves of the molecule of interest are located on an inversion center. Oxygen atoms of the perchlorate counterions and all atoms in the butyronitrile solvent molecules were refined with isotropic displacement parameters. All hydrogen atoms were placed in ideal positions and refined as riding atoms with relative isotropic displacement parameters. All α and β distances for all atoms in the molecule of interest were restrained to be the same using the SAME.⁵ Two of the four perchlorate counterions were disordered and modeled over two positions in a 54:46 and 91:9. All perchlorate counterions were modeled as perfect tetrahedrons using the distance restraint DFIX.⁵ All Cl-O distances were restrained to be equal and freely refined to 1.431 Å and all O-O distances were restrained to be equal and freely refined to 1.431 Å times 1.633, the factor to model the ion as a perfect tetrahedron. Additionally, all α and β distances in the perchlorate counterions were restrained to be the same using the SAME.⁵ The 5.5 butyronitrile solvent molecules were clearly visible on the E-map after full-matrix least squares / difference Fourier cycles were performed. All like bonds of the butyronitrile, C-N, C $_{\alpha}$ -C $_{\beta}$, ect., were set to be equal and allowed to freely refine to a chemically reasonable 1.127, 1.439, 1.494 and 1.516 Å for the bonds in butyronitrile starting from the nitrile bond. Remarkably, the only butyronitrile molecule that was disordered was located on an inversion center and was modeled as over the inversion center in a 50:50 ratio using the Part -1 statement in SHELXL.⁵ The butyronitrile molecules formed a solvent channel throughout the crystal lattice (Figure S5), which likely lead to the instability of the crystals even at low temperature. All overlapping atom pairs were constrained to have the same displacement parameters using the EADP command.⁵

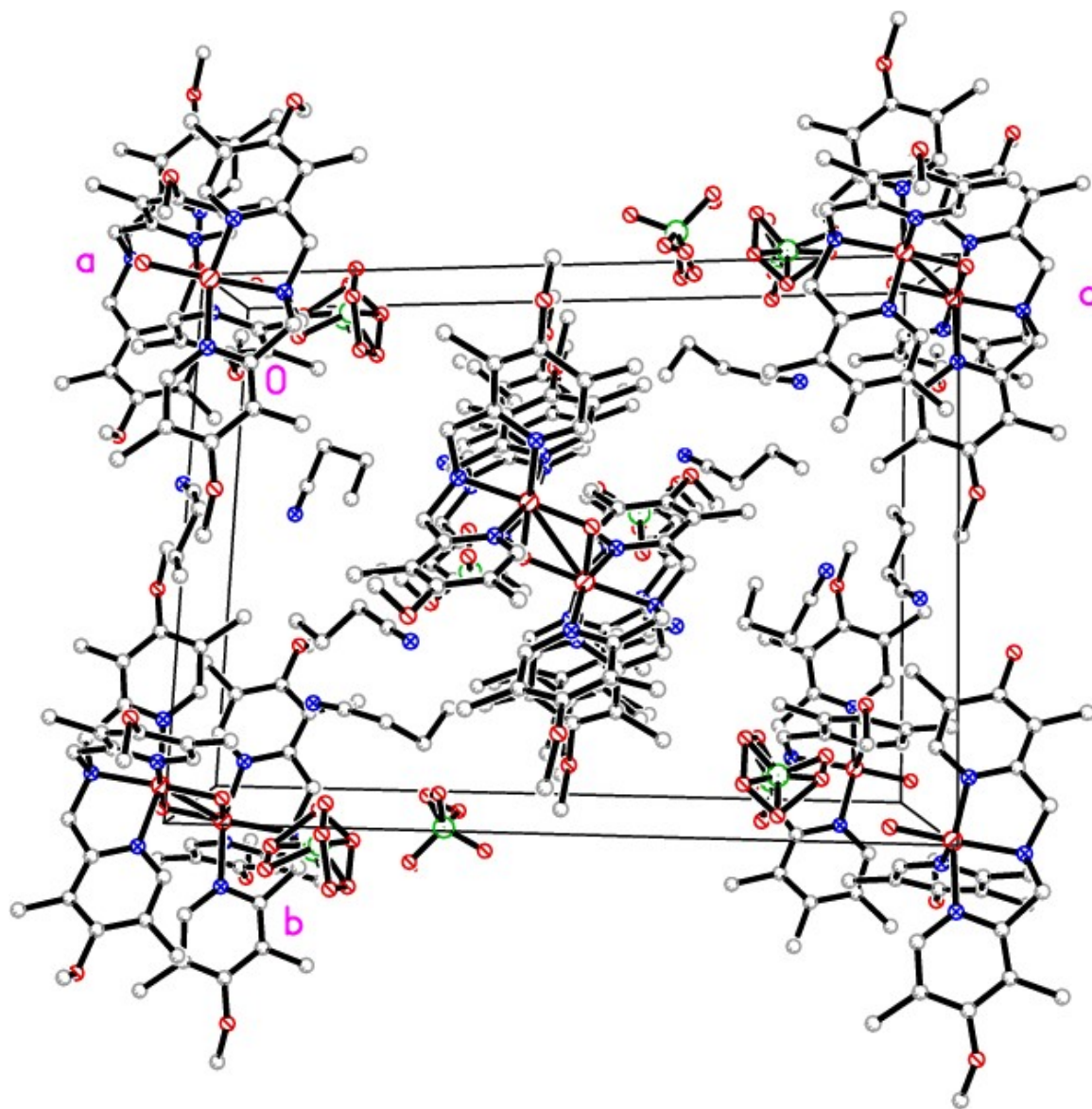


Figure S5: Packing diagram of $[\text{Fe}^{\text{IV}}_2(\mu\text{-O})_2(\text{TPA}^*)_2]^{4+}$ **4A** looking down the a-axis. Hydrogen atoms are removed for clarity. Atoms are drawn at the 50% probability level. The butyronitrile solvent molecules and the perchlorate counterions form a channel surrounding the tetra-cationic compound of interest, likely buffering the large positive charged cations from their neighbors. Atom colors: carbon- gray, oxygen- small red, nitrogen- blue, iron- large red, chlorine- green.

SI References

SI-1: Bruker AXS Inc. APEX2 v2013.6-2. (2013)

SI-2: Bruker AXS Inc. SADABS. (2008)

SI-3: Bruker AXS Inc. SAINT. (2007)

SI-4: Bruker AXS Inc. XPREP. (2008)

SI-5: Sheldrick, G. M. 'A Short History of SHELX', *Acta Crystallogr. Sect. A Found. Crystallogr.* (2008) **A64**, 112-122.

SI-6: Hubschle, C. B., Sheldrick, G. M. and Dittrich B., 'ShelXle: a Qt graphical user interface for SHELXL', *J. Appl. Cryst.* (2011). **44**, 1281-1284.

SI-7: Burla, M. C. *et al.* 'SIR2011: A new package for crystal structure determination and refinement', *J. Appl. Crystallogr.* (2012) **45**, 357-361.